Collective quantum beats from distant multilevel emitters

Ahreum Lee,[1,*] Hyok Sang Han,[1] Fredrik K. Fatemi,[2,3] S. L. Rolston,[1,3] and Kanu Sinha[4]
[1]*Joint Quantum Institute, University of Maryland and the National Institute of Standards and Technology, College Park, Maryland 20742, USA*
[2]*DEVCOM Army Research Laboratory, Adelphi, Maryland 20783, USA*
[3]*Quantum Technology Center, University of Maryland, College Park, Maryland 20742, USA*
[4]*School of Electrical, Computer and Energy Engineering, Arizona State University, Tempe, Arizona 85287, USA*

(Received 15 July 2022; accepted 16 December 2022; published 3 January 2023)

We analyze the dynamics of quantum beats in a system of two V-type three-level atoms coupled to a waveguide. We show that quantum beats can be collectively enhanced or suppressed, akin to Dicke super- and subradiance, depending on the interatomic separation and the initial correlations between the atoms. In particular, the interference properties of the collective beats are determined by the distance between the atoms modulo the beat wavelength. We study the collective atomic and field dynamics, illustrating a crossover from a Markovian to a non-Markovian regime as the atomic separation becomes sufficiently large to bring memory effects of the electromagnetic environment into consideration. In such a non-Markovian regime, collective quantum beats can be enhanced beyond the Markovian limit as a result of retardation effects. Our results demonstrate the rich interplay between multilevel and multiatom quantum interference effects arising in a system of distant quantum emitters.

DOI: 10.1103/PhysRevA.107.013701

I. INTRODUCTION

Quantum beats refer to the quantum interference effect in the radiation emitted from different excited levels in a multilevel atomic system [1]. Similar to the well-known phenomenon of collective atomic spontaneous emission [2], quantum beats can exhibit cooperative effects when considering the fluorescence from a collection of multilevel atoms as demonstrated theoretically [3] and experimentally [4]. Collective effects can thus be a tool for enhancing quantum beats, relevant to improving the sensitivity of precision time-resolved spectroscopy methods [5].

Collective atom-field interactions have been historically explored in systems where atoms are confined within small volumes compared to the resonant wavelengths [6–10]. However, waveguides allow for the realization of cooperative effects between distant emitters, which has been a subject of significant interest in recent theoretical and experimental works [11–22]. In such cases, the radiation emitted from a pair of emitters that are prepared in a symmetric initial state is super(sub)radiant for an interatomic separation that is a (half-)integer multiple of the resonant transition wavelength. Thus the atomic separation (d) modulo the resonant wavelength is crucial in determining the collective emission properties of a system. The interference can thus be engineered in ordered atomic arrays to exhibit strong collective phenomena creating nearly perfect mirrors [23–25] and facilitating quantum metrology [26,27] and quantum memory [13,28].

In this paper, we study the collective quantum beat dynamics of distant multilevel emitters coupled to a waveguide. In such a case, the collective dynamics involves multiple transition frequencies and exhibits even richer interference behavior. We find that at larger length scale the beat wavelength $\lambda_{\text{beat}} \equiv 2\pi v/\omega_{\text{beat}}$ (ω_{beat} being the beat frequency and v being the speed of light in the waveguide) becomes relevant in determining the phase relations between the radiation emitted from different transitions. For a pair of distant multilevel atoms that are prepared in a symmetric initial state with respect to one of the transitions, we show that the resulting quantum beats can be enhanced (suppressed) for an interatomic separation that is a (half-)integer multiple of the beat wavelength, similar to the dependence of Dicke super- and subradiance on the atomic separation modulo the resonant wavelength.

Furthermore, we investigate the regime where the interatomic separation becomes comparable to the coherence length defined as $L_c = v/\Gamma$, where Γ is the characteristic spontaneous emission rate for individual atoms. It has been shown that in such a case the system exhibits rich retardation-induced non-Markovian dynamics, with features such as collective spontaneous emission rates exceeding those of Dicke superradiance [29–32] and formation of highly delocalized atom-photon bound states [32–36]. Increasing the atomic separation to regimes where the retardation effects become relevant, we illustrate a crossover from a Markovian to a non-Markovian dynamics of collective quantum beats.

The paper is organized as follows. We present the model for the system of two V-type three level atoms coupled to a waveguide in Sec. II. Section III analyzes the collective quantum beat dynamics for the atomic and field degrees of freedom. In Sec. IV, we describe the distance dependence of collective quantum beat dynamics. We discuss the conclusions and outlook of the paper in Sec. V.

II. MODEL

We consider two three-level V-type atoms coupled through a one-dimensional waveguide, as shown in the schematic Fig. 1. The ground state is labeled as $|1\rangle$ and the two excited

*alee1206@umd.edu

 ©2023 American Physical Society

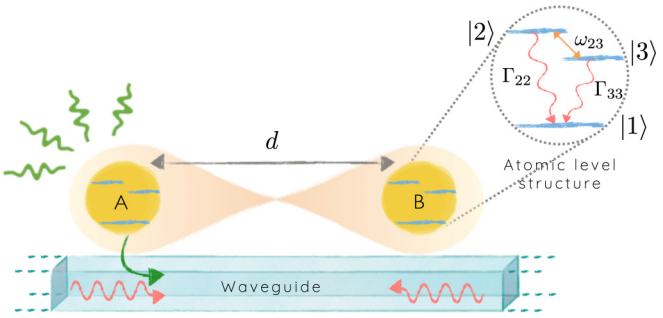

FIG. 1. Schematic representation of two three-level atoms, denoted by A and B, coupled to a waveguide. We consider that each atom has a V-type level structure, with the ground state denoted by $|1\rangle$ and the two excited states denoted by $|2\rangle$ and $|3\rangle$, with decay rates Γ_{22} and Γ_{33}, respectively. The detuning between levels $|2\rangle$ and $|3\rangle$ is ω_{23}. We consider different regimes of the interatomic separation d such that (1) $d \sim \lambda_{\text{beat}} \ll L_c$ and (2) $\lambda_{\text{beat}} \ll d \sim L_c$, with $\lambda_{\text{beat}} = 2\pi v/\omega_{23}$ as the beat wavelength and $L_c = v/\Gamma_{22}$ as the coherence length, with v as the speed of the EM field in the waveguide.

levels are $|2\rangle$ and $|3\rangle$. The frequency difference between levels i and j is denoted as ω_{ij}. The positions of the two atoms are denoted by $x_A = -d/2$ and $x_B = d/2$.

We can write the total Hamiltonian of the system as $H = H_0 + H_{AF}$, where H_0 is the free Hamiltonian and H_{AF} represents the atom-field interaction. The free Hamiltonian is defined as

$$H_0 = \sum_{m=A,B}\sum_{j=2,3} \hbar\omega_{j1}\hat{\sigma}^+_{m,j}\hat{\sigma}^-_{m,j} + \sum_k \hbar\omega_k\left[\hat{a}^\dagger_{R,k}\hat{a}_{R,k} + \hat{a}^\dagger_{L,k}\hat{a}_{L,k}\right]. \tag{1}$$

The first term corresponds to the atomic Hamiltonian where $\hat{\sigma}^\pm_{m,j}$ are the atomic raising and lowering operators acting on the jth level of atom m. The second term is the Hamiltonian for the electromagnetic (EM) field where the creation and annihilation operators $\hat{a}^{(\dagger)}_{R,k}$ and $\hat{a}^{(\dagger)}_{L,k}$ correspond to the right and left propagating field modes with frequency ω_k along the waveguide, respectively. Moving to the interaction picture with respect to H_0, the atom-field interaction Hamiltonian $\tilde{H}_{AF} \equiv e^{iH_0t/\hbar}H_{AF}\,e^{-iH_0t/\hbar}$ is given by

$$\tilde{H}_{AF} = -\sum_{m=A,B}\sum_{j=2,3}\sum_k \hbar g_{m,j}(\omega_k)\left\{\hat{\sigma}^+_{m,j}\left[\hat{a}_{R,k}e^{ikx_m} + \hat{a}_{L,k}e^{-ikx_m}\right]e^{i(\omega_{j1}-\omega_k)t} + \text{H.c.}\right\} \tag{2}$$

where we have employed the rotating-wave approximation. We remark that the waveguide enables the interaction between two distant atoms via a common set of guided modes, without the $\approx 1/r^3$ reduction of interaction strength as in free space. We further assume that the atom-field coupling strengths for the two atoms are equal such that $g_{A,j}(\omega_k) = g_{B,j}(\omega_k) \equiv g_j(\omega_k)$.

We consider a system where the two atoms initially share a single excitation in level 2 and the EM field is in the vacuum state:

$$|\Psi(0)\rangle = \left(\cos\theta|2\rangle_A|1\rangle_B + e^{i\phi}\sin\theta|1\rangle_A|2\rangle_B\right)\otimes|\{0\}\rangle. \tag{3}$$

We remark that even in the absence of an initial superposition of the levels 2 and 3 there is a second-order coupling between the excited levels due to the emission and absorption of virtual photons. Such a second-order coupling allows for the possibility of the initially unpopulated excited level $|3\rangle$ to emit simultaneously with level $|2\rangle$, resulting in vacuum-induced quantum beats [37], as was recently demonstrated experimentally in [4]. Furthermore, the above initial state readily extends to the more general initial state in the single excitation manifold where a single excitation is shared among any of the excited states and any of the two atoms.

Observing that the interaction Hamiltonian preserves the number of excitations in the atom-field system, we make the following ansatz for the time-evolved state:

$$|\Psi(t)\rangle = \left[\sum_{m=A,B}\sum_{j=2,3} c_{m,j}(t)\hat{\sigma}^+_{m,j} + \sum_k\left\{c_R(\omega_k,t)\hat{a}^\dagger_{R,k} + c_L(\omega_k,t)\hat{a}^\dagger_{L,k}\right\}\right]|1\rangle_A|1\rangle_B|\{0\}\rangle. \tag{4}$$

$c_{m,j}(t)$ denotes the excitation amplitude for the mth atom in the jth level and $c_{R(L)}(\omega_k,t)$ stands for the excitation amplitude for the right (left) propagating field mode of frequency ω_k.

III. COLLECTIVE QUANTUM BEAT DYNAMICS

A. Equations of motion

From the interaction Hamiltonian and the single-excitation ansatz for the total system state [Eqs. (2) and (4)], we obtain the equations of motion for the atomic and field excitation amplitudes as follows:

$$\partial_t c_{m,j}(t) = i\sum_k g_j(\omega_k)e^{i(\omega_{j1}-\omega_k)t} \times\left[c_R(\omega_k,t)e^{ikx_m} + c_L(\omega_k,t)e^{-ikx_m}\right], \tag{5}$$

$$\partial_t c_R(\omega_k,t) = i\sum_{m=A,B}\sum_{j=2,3} g_j(\omega_k)e^{-i(\omega_{j1}-\omega_k)t}c_{m,j}(t)e^{-ikx_m}, \tag{6}$$

$$\partial_t c_L(\omega_k,t) = i\sum_{m=A,B}\sum_{j=2,3} g_j(\omega_k)e^{-i(\omega_{j1}-\omega_k)t}c_{m,j}(t)e^{ikx_m}. \tag{7}$$

One can solve for the atomic dynamics by tracing out the field modes assuming a flat spectral density of the EM field such that $g_j(\omega_k) \approx g_j(\omega_{j1}) \equiv g_j$ to obtain

$$\partial_t c_{m,j}(t) = -\sum_{l=2,3}\frac{\Gamma_{jl}}{2}e^{i\omega_{jl}t}c_{m,l}(t) - \sum_{l=2,3}\frac{\eta\Gamma_{jl}}{2}e^{i\omega_{jl}t}e^{i\omega_{l1}\frac{d}{v}}c_{n,l}\left(t-\frac{d}{v}\right)\Theta\left(t-\frac{d}{v}\right), \tag{8}$$

where the atomic indices n and m are not equal and the generalized decay rate Γ_{jl} is defined as

$$\Gamma_{jl} = \frac{d_{j1}d_{l1}\omega^3_{jl}}{3\pi\epsilon_0\hbar v^3}, \tag{9}$$

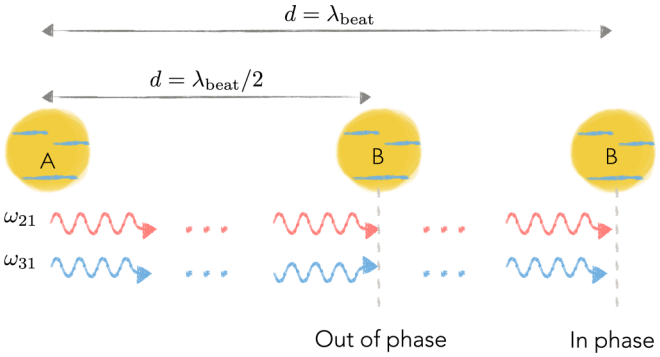

FIG. 2. Schematic representation of the interference between radiation emitted from different atomic transitions for propagation distances of $d = \lambda_{\text{beat}}/2$ and λ_{beat}. The two field modes at different frequencies are in phase right after being emitted and gradually become out of phase as they travel through the waveguide. For a propagation distance of half the beat wavelength, the two modes are exactly out of phase with each other; for a propagation distance equal to the beat wavelength, they become in phase again. Thus, the interatomic distance modulo the beat wavelength determines the interference properties of the radiation emitted from the two transitions.

assuming the transition dipole moments are parallel to each other. We remark that we phenomenologically added the coupling efficiency $\eta \equiv \Gamma_{1D}/\Gamma_{\text{tot}}$, where Γ_{1D} is the decay rate to the waveguide and Γ_{tot} is the total decay rate, in order to account for the decay to the other channels such as free space. The underlying assumption is that spatially separated atoms only interact via guided modes.

One can identify the various processes that contribute to the total collective quantum beat dynamics from Eq. (8) as follows: (1) individual atomic spontaneous emission, corresponding to the terms involving the same atom and same excited level ($n = m,\ j = l$); (2) individual atomic quantum beats, corresponding to the terms involving the same atom and different excited levels ($n = m,\ j \neq l$); (3) collective spontaneous emission, corresponding to the terms with different atoms and same excited levels ($n \neq m,\ j = l$); and (4) collective emission of quantum beats, represented by the interference terms between different atoms and different excited levels ($n \neq m,\ j \neq l$).

The collective atomic and field dynamics is obtained as a combination of the above four processes, exhibiting a rich interplay between different length scales. For example, for a symmetric initial state, (1) when d is a (half-)integer multiple of the transition wavelength λ_{j1}, the photons emitted by the two distant atoms from the respective transitions ($|j\rangle \leftrightarrow |1\rangle$) are in (out of) phase, and (2) when d is a (half-)integer multiple of the beat wavelength λ_{beat}, the two photons of wavelengths λ_{21} and λ_{31} become in (out of) phase at the position of the other atom, as illustrated in Fig. 2.

Furthermore, non-Markovian retardation effects become prominent as the atomic separation becomes comparable to the coherence length of the photons emitted from the atoms. The Markov approximation assumes that the bath correlations decay on a much faster timescale compared to the system relaxation, thus the system evolution only depends on its instantaneous state. In a regime where $d \gtrsim L_c$, the timescale over which the EM field interacts with the delocalized system ($\tau_B \sim d/v$) becomes comparable to the system relaxation timescale ($\tau_R \approx 1/\Gamma_{jj}$). Thus, as $d/v \gtrsim 1/\Gamma_{jj}$, or $\tau_B/\tau_R \gtrsim 1$, it becomes pertinent to include the retardation effects in the EM field mediating the interaction between the two atoms, making the system non-Markovian [32].

B. Atomic dynamics

An arbitrary initial state with a shared single excitation between the two atoms in level $|2\rangle$ [Eq. (3)] can be always decomposed into symmetric($|\psi_+\rangle$) and antisymmetric($|\psi_-\rangle$) states:

$$|\psi_\pm\rangle = \frac{1}{\sqrt{2}}(|2\rangle_A|1\rangle_B \pm |1\rangle_A|2\rangle_B). \tag{10}$$

Thus, we will limit our investigation to the initial states $|\psi_\pm\rangle$. For completeness, the description of a general initial-state case is given in Appendix A.

The time-evolved excitation amplitudes for the two atoms follow the symmetry of the initial state, such that

$$c_{A,j}^{(\pm)}(t) = \pm c_{B,j}^{(\pm)}(t), \tag{11}$$

where the superscripts $+(-)$ correspond to the (anti)symmetric initial states $|\psi_\pm\rangle$. Importantly, we note that the symmetry of the atomic state with respect to both the $|3\rangle \leftrightarrow |1\rangle$ and the $|2\rangle \leftrightarrow |1\rangle$ transitions is the same as the initial symmetry for the $|2\rangle \leftrightarrow |1\rangle$ transition throughout the dynamics.

To simplify the notation, we will drop the atomic labels m, i.e., $c_{A,j}^{(\pm)}(t) \equiv c_j^{(\pm)}(t)$, and focus on the evolution of atom A. From solving the coupled atomic dynamical equations of motion in Eq. (8) by taking a Laplace transform, one obtains the atomic dynamics as the sum of various modes (see Appendix A for details):

$$c_2^{(\pm)}(t) = \sum_{n=-\infty}^{\infty} \alpha_n^{(\pm)} e^{s_n^{(\pm)} t}, \tag{12}$$

$$c_3^{(\pm)}(t) = \sum_{n=-\infty}^{\infty} \beta_n^{(\pm)} e^{(s_n^{(\pm)} - i\omega_{23})t}. \tag{13}$$

The coefficients $s_n^{(\pm)}$ and $s_n^{(\pm)} - i\omega_{23}$ denote the characteristic complex eigenfrequencies of the amplitude dynamics for the levels 2 and 3, respectively, and are defined as the poles of the propagator $G^{(\pm)}(s)$:

$$G^{(\pm)}(s) \equiv \Bigg[\left(s - i\omega_{23} + \frac{\Gamma_{33}}{2} \pm \eta\frac{\Gamma_{33}}{2}e^{i\phi_2}e^{-\frac{d}{v}s}\right) \times \left(s + \frac{\Gamma_{22}}{2} \pm \eta\frac{\Gamma_{22}}{2}e^{i\phi_2}e^{-\frac{d}{v}s}\right) - \frac{\Gamma_{23}\Gamma_{32}}{4}\left(1 \pm \eta e^{i\phi_2}e^{-\frac{d}{v}s}\right)^2\Bigg]^{-1}. \tag{14}$$

Here, $\phi_2 = \omega_{21}d/v$ is the propagation phases for the resonant transition frequency ω_{21}. In general, the propagator above has an infinite number of poles, and it is difficult to express the corresponding eigenfrequencies in a closed-form analytical solution. We therefore obtain $s_n^{(\pm)}$ numerically for

a finite number of poles of the propagator $G^{(\pm)}(s_n^{(\pm)})$ with $n \in \{-N, \ldots, N\}$.

The corresponding coefficients $\alpha_n^{(\pm)}$ and $\beta_n^{(\pm)}$ for the nth eigenfrequency are

$$\alpha_n^{(\pm)} = \frac{1}{\sqrt{2}} \lim_{s \to s_n} \frac{s - i\omega_{23} + \frac{\Gamma_{33}}{2} \pm \eta \frac{\Gamma_{33}}{2} e^{i\phi_2} e^{-\frac{d}{v}s}}{\partial_s \left\{ [G^{(\pm)}(s)]^{-1} \right\}}, \tag{15}$$

$$\beta_n^{(\pm)} = -\frac{\Gamma_{32}}{2\sqrt{2}} \lim_{s \to s_n} \frac{\left(1 \pm \eta e^{i\phi_2} e^{-\frac{d}{v}s}\right)}{\partial_s \left\{ [G^{(\pm)}(s)]^{-1} \right\}}. \tag{16}$$

In the limit where atoms are colocated, the eigenfrequencies given by the poles of the propagator [Eq. (14)] can be solved analytically, and the atomic dynamics corresponds to simple collective quantum beat dynamics without delay. We remark that when the atoms are colocated different atoms may interact via the free space as well as the guided field modes, thus the effective coupling efficiency for this specific case should be set to 1. Generally, when the atoms are close enough so that they may interact through the free space mode, the coupling efficiency should change accordingly. For the symmetric initial state, this yields two solutions: $s^{(+)} = \{-\frac{\Gamma_{22}+\Gamma_{33}}{2} + i\frac{\omega_{23}+\delta}{2}, -\frac{\Gamma_{22}+\Gamma_{33}}{2} + i\frac{\omega_{23}-\delta}{2}\}$ where $\delta = [{\omega_{23}}^2 - (\Gamma_{22} + \Gamma_{33})^2 - 2i\omega_{23}(\Gamma_{22} - \Gamma_{33})]^{\frac{1}{2}}$. In the regime where the excited levels are well separated ($\frac{\Gamma_{ij}}{\omega_{23}} \ll 1$), the atomic dynamics can be simplified as follows:

$$c_2^{(+)}(t) = \frac{1}{\sqrt{2}} \left[e^{-\Gamma_{22}t} - \left(\frac{\Gamma_{32}\Gamma_{23}}{{\omega_{23}}^2} \right) e^{-\Gamma_{33}t} e^{i\omega_{23}t} \right], \tag{17}$$

$$c_3^{(+)}(t) = \frac{i\Gamma_{32}}{\sqrt{2}\omega_{23}} \left[e^{-\Gamma_{33}t} - e^{-\Gamma_{22}t} e^{-i\omega_{23}t} \right]. \tag{18}$$

The dynamics of the amplitude of level 2 is dominated by the collective decay at a rate Γ_{22}, overlaid with a beating term with an amplitude $\Gamma_{32}\Gamma_{23}/\omega_{23}^2 \ll 1$. The initial population in level 3 being zero, the excitations in level 3 arise exclusively from a second-order vacuum-induced coupling between level 2 and level 3. Thus, the decay and the beat terms in $c_3(t)$ have the same amplitude.

For the antisymmetric initial state in the zero-distance case we obtain the complex eigenfrequencies as $s^{(-)} = \{0, i\omega_{23}\}$, without any real component or decay. Thus, the system remains in the subradiant state with no evolution of the corresponding atomic coefficients: $c_2^{(-)}(t) = \frac{1}{\sqrt{2}}$, $c_3^{(-)}(t) = 0$.

C. Field dynamics

While the atomic dynamics provides physical intuition, it cannot be measured directly in experiments. Instead, one measures the intensity of the light emitted from the system, which carries indirect information about the atomic dynamics. The intensity emitted by the atomic system is given by $I(x,t) = \frac{\epsilon_0 c}{2} \langle \psi(t) | \hat{E}^\dagger(x,t) \hat{E}(x,t) | \psi(t) \rangle$, with the electric-field operator defined as $\hat{E}(x,t) = \int_0^\infty dk \mathcal{E}_k [\hat{a}_{R,k} e^{ikx} + \hat{a}_{L,k} e^{-ikx}] e^{-i\omega_k t}$. This can be calculated explicitly as follows (see Appendix B for details):

$$I(x,t)/I_0 = \left| \sum_{j=2,3} \sum_{m=A,B} \frac{g_j}{g_2} \left\{ \underbrace{c_{m,j}\left(t - \frac{x - x_m}{v}\right) e^{-i\omega_{j1}\left(t - \frac{x-x_m}{v}\right)} \left[\Theta\left(t - \frac{x-x_m}{v}\right) - \Theta\left(-\frac{x-x_m}{v}\right) \right]}_{\text{Right light cone for atom } m \text{ at frequency } \omega_{j1}} \right. \right.$$

$$\left. \left. + \underbrace{c_{m,j}\left(t + \frac{x - x_m}{v}\right) e^{-i\omega_{j1}\left(t + \frac{x-x_m}{v}\right)} \left[\Theta\left(t + \frac{x-x_m}{v}\right) - \Theta\left(\frac{x-x_m}{v}\right) \right]}_{\text{Left light cone for atom } m \text{ at frequency } \omega_{j1}} \right\} \right|^2. \tag{19}$$

The first and second terms in the above expression appear in terms of $t \pm (x - x_m)/v$, corresponding to the light cone emitted by atom m at frequency ω_{j1} towards right and left, respectively. Before the two light cones meet, the atoms are causally disconnected and emit independently. As each atom "sees" the other atom, the interference between the light cones at the two transition frequencies emitted by the two atoms leads to collective quantum beat dynamics.

The intensity measured outside the system ($x < x_A$ or $x > x_B$) can be expressed in a further simplified form by taking the limit $x \to x_B^+$ and making use of the system eigenfrequencies:

$$I(t)/I_0 = \left| \sum_n \left(\alpha_n^{(\pm)} + \frac{g_3}{g_2} \beta_n^{(\pm)} \right) \right.$$

$$\left. \times \left(\Theta(t) \pm e^{-s_n^{(\pm)} d/v} \Theta(t - d/v) \right) e^{s_n^{(\pm)} t} \right|^2. \tag{20}$$

From the above expression we note that quantum beats result from the interference of the modes with different frequencies, such that $\mathrm{Im}s_n^{(\pm)} \neq \mathrm{Im}s_m^{(\pm)}$. In particular, collective quantum beats originate from the interference between the fields emitted by the two atoms at different frequencies for $t > d/v$. The collective beat amplitude has a distance dependence as can be seen from the prefactor $e^{-s_n^{(\pm)} d/v}$, which corresponds to the difference in phase and amplitude for various field modes as they propagate between the two atoms.

In the limit of two coincident atoms ($d \to 0$), the intensity measured at $x \to x_B^+$ is

$$I(t)/I_0 = \left| c_{A2}(t) + \frac{g_3}{g_2} c_{A3}(t) e^{i\omega_{23}t} \right.$$

$$\left. + c_{B2}(t) + \frac{g_3}{g_2} c_{B3}(t) e^{i\omega_{23}t} \right|^2 \Theta(t). \tag{21}$$

TABLE I. Summary of parameters used in calculations, based on typical values in a superconducting circuit setup. The frequencies are in the units of Γ_{22}, and the lengths are in units of v/Γ_{22}.

Decay rate of level 3 (Γ_{33}/Γ_{22})	1
Energy separation of level 2 and 3 (ω_{23}/Γ_{22})	50
Resonant frequency of level 2 (ω_{21}/Γ_{22})	10^4
Coherence length ($L_c \times \Gamma_{22}/v$)	1
Beat wavelength ($\lambda_{\text{beat}} \times \Gamma_{22}/v$)	$4\pi \times 10^{-2}$
Transition wavelength ($\lambda_{21} \times \Gamma_{22}/v$)	$2\pi \times 10^{-4}$

For the antisymmetric initial state where $c_{A2}(t) = -c_{B2}(t)$ and $c_{A3}(t) = -c_{B3}(t)$, the total emitted intensity vanishes, as expected for a Dicke subradiant state.

For a symmetric initial state where $c_{A2}(t) = c_{B2}(t)$ and $c_{A3}(t) = c_{B3}(t)$, the emitted intensity is four times that of a single three-level atom, corresponding to standard Dicke superradiance. Plugging in Eqs. (17) and (18) into Eq. (21), one gets

$$I(t)/I_0 = e^{-2\Gamma_{22}t} + \frac{\Gamma_{33}}{\Gamma_{22}}\left(\frac{\Gamma_{23}\Gamma_{32}}{{\omega_{23}}^2}\right)e^{-2\Gamma_{33}t} - 2\frac{\Gamma_{23}\Gamma_{32}}{\omega_{23}\Gamma_{22}}\sin(\omega_{23}t)e^{-(\Gamma_{22}+\Gamma_{33})t}, \quad (22)$$

using the relation ${g_j}^2 \propto \Gamma_{jj}$. The first two terms correspond to spontaneous emission from levels 2 and 3, and the third term represents quantum beats. The above expression is in agreement with the collective quantum beat dynamics from coincident atoms as previously obtained in [4].[1]

IV. DISTANCE DEPENDENCE OF COLLECTIVE QUANTUM BEAT DYNAMICS

We now present the system dynamics for a specific implementation of the model in a superconducting circuit setup as an example [21,38], with parameters described in Table I. As superconducting circuits allow for both a strong enough coupling between the emitters and field, as well as a precise control of emitter positions, the parameters can be preferentially chosen to best observe the collective quantum beat dynamics. For example, the ratio $\sim\Gamma_{23}/\omega_{23}$ can be sufficiently large so that the vacuum-induced coupling between the excited levels results in sizable quantum beats [Eq. (22)]. Unlike in the case of optical frequencies, the transition wavelengths being in the microwave regime enables a precise enough positioning of emitters such that one can realize the desired separations needed to observe various interference phenomena in collective quantum beats. Also, the ratio of the characteristic wavelengths (transition and beat wavelengths) to the coherence length, while being small, is still substantial enough compared to optical regimes to allow one to access both the Markovian and non-Markovian regimes of the system dynamics with a small variation of the emitter separation d. We note that, as long as the parameters are carefully chosen regarding the above requirements, the various interference properties of collective quantum beats should appear in any multilevel quantum system.

In particular we discuss the dependence of the collective system dynamics on atomic separation across two different regimes wherein (1) $d \ll L_c$ (Markovian regime) and (2) $d \gtrsim L_c$ (non-Markovian regime). In each of these regimes, we analyze the system dynamics for the symmetric and antisymmetric initial states of the two artificial atoms [Eq. (10)], considering interatomic separations of integer and half-integer multiples of the beat wavelength. For simplicity we assume that d is an integer multiple of λ_{21}. While the initial state determines the total collective spontaneous emission, the interatomic distance modulo the beat wavelength determines the interference properties of the collective quantum beats, as discussed in Sec. III A.

A. Markovian regime

We study the dynamics of atomic excitation probabilities and the field intensity for interatomic separations of $d = \{\lambda_{\text{beat}}, \lambda_{\text{beat}}/2\} \ll L_c$. We numerically calculate the poles of Eq. (14) for $|\text{Re}[s_n^{(j,\pm)}]| < 200\,\Gamma_{22}$ and $|\text{Im}[s_n^{(j,\pm)}]| < 200\,\omega_{23}$. Including sufficient high-frequency modes allows one to correctly capture the dynamics of the system for the timescales of interest (see Appendix C for details).

Figure 3 depicts the atomic and field dynamics for initial symmetric and antisymmetric states of the two atoms. We note that the onset of collective dynamics happens at $d = \lambda_{\text{beat}}$ or $\frac{1}{2}\lambda_{\text{beat}}$ depending on the interatomic separation as indicated by the vertical dash-dotted lines. Figures 3(a) and 3(b) illustrate the level 2 population dynamics which exhibits a super(sub)radiant decay for (anti)symmetric initial states. It can be seen from Eq. (17) that the amplitude of the beat term is smaller compared to that of the individual decay in level 2 dynamics by a factor of $\Gamma_{23}\Gamma_{32}/{\omega_{23}}^2 \ll 1$. Thus, we do not see any visible beats in the level 2 population curves.

More interestingly, Figs. 3(c) and 3(d) illustrate the collective quantum beat effect as seen in the level 3 population dynamics. We note that for an interatomic separation of $d = \lambda_{\text{beat}}$ there is a collective enhancement of the quantum beats for the symmetric initial state, and suppression for the antisymmetric initial state as denoted in Fig. 3(c). For this separation, the phase of the field modes mediating the interaction between the atoms is an even integer multiple of 2π such that $\omega_{21}d/v = 2n\pi$, $\omega_{31}d/v = 2m\pi$ $(\{n, m\} \in \mathbb{N})$. Furthermore, the total atomic state is (anti)symmetric with respect to the $|3\rangle \leftrightarrow |1\rangle$ transition for an initial (anti)symmetric state with respect to the $|2\rangle \leftrightarrow |1\rangle$ transition. Thus, we observe an enhancement or suppression of the quantum beats for an initial symmetric or antisymmetric state, respectively. More specifically, it can be seen that the amplitude of the first peak of the collective "superradiant" quantum beats (solid blue) is enhanced roughly by a factor of $\approx$4.1 in comparison with the

[1]While, strictly speaking, the experiment in [4] corresponds to a timed Dicke state of a finite-sized ensemble, it can be approximated well by a symmetric state of coincident atoms. Such an assumption is valid in the limit where the ensemble size ($\approx$2 mm) is much smaller compared to the beat wavelength ($\approx$2.5 m). We further remark that the dynamics of a timed Dicke state of atoms separated by a distance comparable to λ_{beat} is different from that of the symmetric state of coincident atoms because every $\frac{1}{2}\lambda_{\text{beat}}$ the photons of two different frequencies would be out of phase.

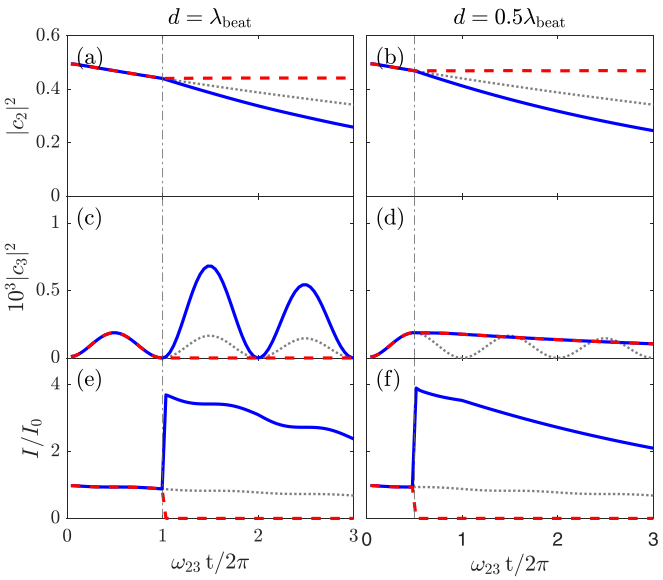

FIG. 3. Atom-field dynamics in the Markovian regime: (a), (b) level 2 dynamics, (c), (d) level 3 dynamics, and (e), (f) field dynamics measured at $x \to x_B^+$ for interatomic separations (a), (c), (e) $d = \lambda_{\text{beat}}$ and (b), (d), (f) $d = \frac{1}{2}\lambda_{\text{beat}}$. The solid blue curves are for the symmetric initial state, and the dashed red curves are for the antisymmetric initial state. The vertical dash-dotted lines indicate the times when the field emitted from one atom reaches the other atom. For comparison the single atom dynamics is drawn with the dotted gray lines. The level 3 population is scaled by a factor of 10^3 for clarity of illustration.

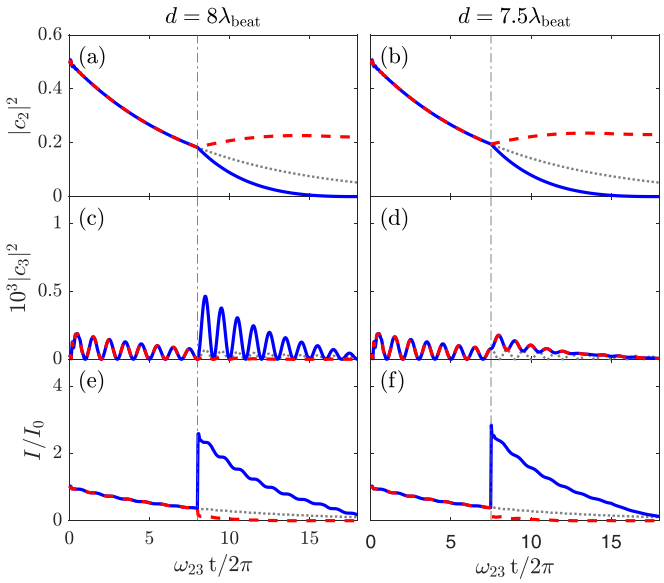

FIG. 4. Non-Markovian regime: (a), (b) level 2 dynamics, (c), (d) level 3 dynamics, and (e), (f) field dynamics measured at $x \to x_B^+$ for interatomic separations (a), (c), (e) $d = 8\lambda_{\text{beat}}$ and (b), (d), (f) $d = 7.5\lambda_{\text{beat}}$. The solid blue curves are for the symmetric initial state, and the dashed red curves are for the antisymmetric initial state. The vertical dashed-dotted lines indicate the times when the field emitted from one atom reaches the other atom. For comparison the single atom dynamics is drawn with the dotted gray lines. The level 3 population is scaled by a factor of 10^3.

independent emission case (dotted gray). In contrast, it can be seen in Fig. 3(d) that for a separation of $d = \lambda_{\text{beat}}/2$ the resulting beats are suppressed as a result of the destructive interference between the fields emitted from the two atoms at ω_{21} and ω_{31}, as illustrated in Fig. 2.

In Figs. 3(e) and 3(f), the intensity of the light measured outside the system is depicted. The radiated intensity, as given by Eq. (19), is governed by the interference between the atomic excitation amplitudes. For the (anti)symmetric initial state, the overall emission is superradiant (subradiant). For the case of superradiant emission, the size of the beat is enhanced (suppressed) for an atomic separation of $d = \lambda_{\text{beat}}$ ($d = \frac{1}{2}\lambda_{\text{beat}}$), in agreement with the collective atomic dynamics.

B. Non-Markovian regime

We now consider the case wherein the atomic separations are comparable to the coherence length of the emitted photons, with $d = 7.5\lambda_{\text{beat}} \approx 0.94L_c$ and $8\lambda_{\text{beat}} \approx L_c$. We note that for such large separations the retardation effects of the waveguide field become relevant, rendering the system dynamics non-Markovian. We calculate the dynamics numerically by obtaining the characteristic system frequencies as the poles of the propagator Eq. (14) within $|\text{Re}[s_n^{(j,\pm)}]| < 10\,\Gamma_{22}$ and $|\text{Im}[s_n^{(j,\pm)}]| < 10\,\omega_{23}$ (see Appendix C for details).

The atomic and field dynamics for this regime is shown in Fig. 4 for the initial symmetric and antisymmetric states. The level 2 dynamics for a symmetric initial state as denoted by the solid blue curves in Figs. 4(a) and 4(b) exhibits collective emission rates faster than standard Dicke superradiance, which is termed "superduperradiance" (see Appendix D for comparison of decay profiles of superduperradiance and Dicke superradiance), similar to the non-Markovian collective dynamics for a system of two two-level atoms [29,32,39]. Such an enhancement of the collective decay rate can be understood by considering the atomic collective emission in terms of a mutually stimulated emission process wherein each atomic dipole is stimulated by the field emitted by the other atom [31,40]. As each atom emits into the waveguide, there is a probability amplitude associated with the emitted field reaching the other atom—in the presence of delay this amplitude increases with the atomic separation, causing an enhancement in the instantaneous rate of collective emission beyond regular superradiance. For an antisymmetric initial state (dashed red curves), one can see the formation of delocalized atom-photon bound states in continuum in agreement with previous studies in delocalized two-level emitters [33,34]. Such atom-photon bound states arise as a result of the destructive interference between the atomic dipole and the fields emitted by each of the atoms, which causes the fields to be reflected as they interact with the atoms.

The effects of retardation on collective quantum beats are illustrated in the population dynamics of level 3 in Figs. 4(c) and 4(d). For an interatomic separation $d = 8\lambda_{\text{beat}}$ as seen in Fig. 4(c), we observe an enhancement of the quantum beats for a symmetric initial state and moderate suppression of beats for the antisymmetric initial state. Furthermore, comparing the first peak of the collective quantum beats (solid blue)

with that of the independent decay (dotted gray) shows an enhancement beyond the Markovian case by roughly a factor of ≈6.8. For a separation of $d = 7.5\lambda_{\text{beat}}$ as illustrated in Fig. 4(d), the population dynamics of level 3 for both the initial symmetric and antisymmetric cases exhibits beating in addition to an exponential decay.

The light intensity measured outside the system is depicted in Figs. 4(e) and 4(f). The symmetric initial state exhibits an overall exponential decay faster than Dicke superradiance, with an overlaid beating that is enhanced (suppressed) for a separation $d = 8\lambda_{\text{beat}}$ ($d = 7.5\lambda_{\text{beat}}$). The antisymmetric initial state shows a suppressed total emission outside the system, indicating that most of the light is trapped in between the atoms forming a delocalized atom-photon bound state. We note that the atom-photon bound state in this case has a larger photonic amplitude than in the Markovian case. However, there is a finite emission into the field modes from the otherwise subradiant state, indicating existence of additional modes in a non-Markovian regime that provide channels for the atomic excitations to decay away. Such modes have been previously investigated in the context of the steady-state atomic spectrum emitted from two distant two-level atoms [31].

V. DISCUSSION

In this paper we have demonstrated the distance-dependent dynamics of collective quantum beats, resulting from the interference between the radiation emitted from a collection of multilevel atoms coupled to a waveguide. Considering a system of two V-type three-level atoms interacting via a waveguide, we show that the coherent interference between the spontaneous emission from different excited levels of the two atoms results in a collective quantum beat phenomenon [4] (Sec. II). We find that the distance between the atoms modulo the beat wavelength (d/λ_{beat}) is critical in determining the interference properties of such collective quantum beats: the emitted fields at the two transition frequencies go from interfering constructively to interfering destructively for $d = n\lambda_{\text{beat}}$ to $(n + 1/2)\lambda_{\text{beat}}$ (Fig. 2). We obtain the collective dynamics of the total atom-field system by analyzing the system in terms of its characteristic complex eigenfrequencies determined by the poles of the system propagator (Sec. III). In the limit $d \to 0$ our results agree with the recent experimental investigations of vacuum-induced collective quantum beats from a small sample, which could be approximately considered as a system of coincident atoms [4]. A general analysis of the collective atomic and field dynamics as a function of the interatomic separation and the initial atomic states is presented in Sec. IV. We find that while the atomic separation modulo the transition wavelength in conjunction with the symmetry properties of the initial state governs the overall collective spontaneous emission the length scale λ_{beat} governs the collective nature of the quantum beats. We further investigate the non-Markovian dynamics of collective quantum beats in Sec. IV B. As the system size become comparable to the coherence length of the emitted photons ($d \sim v/\Gamma$), there can be significant retardation effects in the field mediating the interaction between the atoms, rendering the system dynamics non-Markovian. In such a regime, we find that the collective quantum beats can exhibit a non-Markovian enhancement beyond superradiant quantum beats arising in the Markovian regime, as illustrated in Fig. 4.

The results presented in this paper open directions for investigating and controlling radiation from multilevel atomic systems coupled to waveguides. Quantum beats are relevant to precision time-resolved spectroscopy measurements [5]; a collective enhancement of quantum beats can improve sensitivities of such measurements. It would be pertinent to extend the present model to a system of N atoms for characterizing the metrological advantage offered by the collective nature of quantum beats.

Furthermore, collections of quantum emitters coupled to waveguides are a paradigmatic system for implementation of quantum networks and long-distance quantum communication protocols. It has been shown that collective multilevel atomic systems offer a higher-dimensional entangled state space, enabling efficient quantum memories [41] and secure quantum communication [42–44]. Our analysis is relevant to such schemes, with a consideration of retardation effects, which can be significant in distributed quantum information processing.

ACKNOWLEDGMENTS

We thank Pablo Solano, Mohammad Hafezi, and Deniz Kurdak for helpful discussions. This research was supported by the Maryland ARL Quantum Partnership (Grant No. W911NF-19-2-0181) and Joint Quantum Institute (Grant No. 70NANB16H168).

APPENDIX A: ATOMIC DYNAMICS

We can solve the coupled atomic equations of motion [Eq. (8)] by using Laplace transformation. Defining Laplace-transformed coefficients, $\tilde{c}_{m,j}(s) \equiv \int_0^\infty c_{m,j}(t)e^{-st}dt$, Eq. (8) reads

$$\partial_t c_{m,j}(t) = -\sum_{l=2,3} \frac{\Gamma_{jl}}{2}\tilde{c}_{m,l}(s - i\omega_{jl}) - \sum_{l=2,3} \frac{\eta\Gamma_{jl}}{2} e^{-\frac{d}{v}(s-i\omega_{j1})}\tilde{c}_{n,l}(s - i\omega_{jl}), \tag{A1}$$

where $m \neq n$. Setting the initial-state condition [Eq. (3)], we get the coupled equations in Laplace space:

$$s\tilde{c}_{A2}(s) = \cos\theta - \frac{\Gamma_{22}}{2}\tilde{c}_{A2}(s) - \frac{\Gamma_{23}}{2}\tilde{c}_{A3}(s - i\omega_{23}) - \frac{\Gamma_{22}}{2}\eta e^{i\phi_2}e^{-\frac{d}{v}s}\tilde{c}_{B2}(s) - \frac{\Gamma_{23}}{2}\eta e^{i\phi_2}e^{-\frac{d}{v}s}\tilde{c}_{B3}(s - i\omega_{23}), \tag{A2a}$$

$$s\tilde{c}_{B2}(s) = e^{i\phi}\sin\theta - \frac{\Gamma_{22}}{2}\eta e^{i\phi_2}e^{-\frac{d}{v}s}\tilde{c}_{A2}(s) - \frac{\Gamma_{23}}{2}\eta e^{i\phi_2}e^{-\frac{d}{v}s}\tilde{c}_{A3}(s - i\omega_{23}) - \frac{\Gamma_{22}}{2}\tilde{c}_{B2}(s) - \frac{\Gamma_{23}}{2}\tilde{c}_{B3}(s - i\omega_{23}), \tag{A2b}$$

$$s\tilde{c}_{A3}(s) = -\frac{\Gamma_{32}}{2}\tilde{c}_{A2}(s+i\omega_{23}) - \frac{\Gamma_{33}}{2}\tilde{c}_{A3}(s) - \frac{\Gamma_{32}}{2}\eta e^{i\phi_3}e^{-\frac{d}{v}s}\tilde{c}_{B2}(s+i\omega_{23}) - \frac{\Gamma_{33}}{2}\eta e^{i\phi_3}e^{-\frac{d}{v}s}\tilde{c}_{B3}(s), \tag{A2c}$$

$$s\tilde{c}_{B3}(s) = -\frac{\Gamma_{32}}{2}\eta e^{i\phi_3}e^{-\frac{d}{v}s}\tilde{c}_{A2}(s+i\omega_{23}) - \frac{\Gamma_{33}}{2}\eta e^{i\phi_3}e^{-\frac{d}{v}s}\tilde{c}_{A3}(s) - \frac{\Gamma_{32}}{2}\tilde{c}_{B2}(s+i\omega_{23}) - \frac{\Gamma_{33}}{2}\tilde{c}_{B3}(s). \tag{A2d}$$

Here, $\phi_j = \omega_{j1}d/v$ is the general propagation phase for a photon of frequency ω_{j1}. First solving for $\tilde{c}_{A2}(s)$ and $\tilde{c}_{B2}(s)$, we get

$$\tilde{c}_{A2}(s) = \frac{\cos\theta\, A(s) - e^{i\phi}\sin\theta\, B(s)}{C(s)},$$
$$\tilde{c}_{B2}(s) = \frac{e^{i\phi}\sin\theta\, A(s) - \cos\theta\, B(s)}{C(s)}, \tag{A3}$$

where $A(s)$, $B(s)$, $C(s)$, and $D(s)$ are defined as

$$\begin{aligned}
A(s) &= \left(s - i\omega_{23} + \frac{\Gamma_{33}}{2}\right)\left[\left(s+\frac{\Gamma_{22}}{2}\right)\left(s - i\omega_{23} + \frac{\Gamma_{33}}{2}\right) - \frac{\Gamma_{23}\Gamma_{32}}{4}\right] \\
&\quad - \eta^2 e^{2i\phi_2}e^{-2\frac{d}{v}s}\left[\left(\frac{\Gamma_{33}}{2}\right)^2\left(s+\frac{\Gamma_{22}}{2}\right) + \frac{\Gamma_{23}\Gamma_{32}}{4}\left(s - i\omega_{23} - \frac{\Gamma_{33}}{2}\right)\right], \\
B(s) &= \eta e^{i\phi_2}e^{-\frac{d}{v}s}\left[\frac{\Gamma_{22}}{2}\left(s - i\omega_{23} + \frac{\Gamma_{33}}{2}\right)^2 - \frac{\Gamma_{23}\Gamma_{32}}{4}\left(2s - 2i\omega_{23} + \frac{\Gamma_{33}}{2}\right)\right] - \eta^3 e^{3i\phi_2}e^{-3\frac{d}{v}s}\frac{\Gamma_{33}}{2}\left[\frac{\Gamma_{22}\Gamma_{33}}{4} - \frac{\Gamma_{23}\Gamma_{32}}{4}\right], \\
C(s) &= \left[\left(s - i\omega_{23} + \frac{\Gamma_{33}}{2} + \frac{\Gamma_{33}}{2}\eta e^{i\phi_2}e^{-\frac{d}{v}s}\right)\left(s + \frac{\Gamma_{22}}{2} + \frac{\Gamma_{22}}{2}\eta e^{i\phi_2}e^{-\frac{d}{v}s}\right) - \frac{\Gamma_{23}\Gamma_{32}}{4}\left(1 + \eta e^{i\phi_2}e^{-\frac{d}{v}s}\right)^2\right] \\
&\quad \times \left[\left(s - i\omega_{23} + \frac{\Gamma_{33}}{2} - \frac{\Gamma_{33}}{2}\eta e^{i\phi_2}e^{-\frac{d}{v}s}\right)\left(s + \frac{\Gamma_{22}}{2} - \frac{\Gamma_{22}}{2}\eta e^{i\phi_2}e^{-\frac{d}{v}s}\right) - \frac{\Gamma_{23}\Gamma_{32}}{4}\left(1 - \eta e^{i\phi_2}e^{-\frac{d}{v}s}\right)^2\right].
\end{aligned} \tag{A4}$$

Then $\tilde{c}_{A3}(s)$ and $\tilde{c}_{B3}(s)$ are obtained in terms of $\tilde{c}_{A2}(s)$ and $\tilde{c}_{B2}(s)$:

$$\tilde{c}_{A3}(s) = -\frac{\Gamma_{32}}{2}\frac{\left(s + \frac{\Gamma_{33}}{2} - \frac{\Gamma_{33}}{2}\eta^2 e^{2i\phi_3}e^{-2\frac{d}{v}s}\right)\tilde{c}_{A2}(s+i\omega_{23}) + s\eta e^{i\phi_3}e^{-\frac{d}{v}s}\tilde{c}_{B2}(s+i\omega_{23})}{\left(s+\frac{\Gamma_{33}}{2}\right)^2 - \left(\frac{\Gamma_{33}}{2}\right)^2\eta^2 e^{2i\phi_3}e^{-2\frac{d}{v}s}},$$
$$\tilde{c}_{B3}(s) = -\frac{\Gamma_{32}}{2}\frac{s\eta e^{i\phi_3}e^{-\frac{d}{v}s}\tilde{c}_{A2}(s+i\omega_{23}) + \left(s + \frac{\Gamma_{33}}{2} - \frac{\Gamma_{33}}{2}\eta^2 e^{2i\phi_3}e^{-2\frac{d}{v}s}\right)\tilde{c}_{B2}(s+i\omega_{23})}{\left(s+\frac{\Gamma_{33}}{2}\right)^2 - \left(\frac{\Gamma_{33}}{2}\right)^2\eta^2 e^{2i\phi_3}e^{-2\frac{d}{v}s}}. \tag{A5}$$

We first numerically find the poles s_n of the denominators in Eqs. (A3) and (A5), with each pole representing a complex eigenfrequency of the system. The excitation amplitude $\tilde{c}(s)$ in Laplace space is expressed in terms of its modes:

$$\tilde{c}(s) = \sum_n \frac{w_n}{s - s_n}, \tag{A6}$$

where $w_n = \lim_{s\to s_n}(s - s_n)\tilde{c}(s)$.

In this paper we consider two specific initial states: a symmetric and antisymmetric superposition of a single excitation in level 2. For the symmetric initial state, i.e., $\theta = \pi/4$ and $\phi = 0$,

$$\tilde{c}_{A2}(s) = \tilde{c}_{B2}(s) = \frac{1}{\sqrt{2}}\frac{s - i\omega_{23} + \frac{\Gamma_{33}}{2} + \frac{\Gamma_{33}}{2}\eta e^{i\phi_2}e^{-\frac{d}{v}s}}{\left(s - i\omega_{23} + \frac{\Gamma_{33}}{2} + \frac{\Gamma_{33}}{2}\eta e^{i\phi_2}e^{-\frac{d}{v}s}\right)\left(s + \frac{\Gamma_{22}}{2} + \frac{\Gamma_{22}}{2}\eta e^{i\phi_2}e^{-\frac{d}{v}s}\right) - \frac{\Gamma_{23}\Gamma_{32}}{4}(1 + \eta e^{i\phi_2}e^{-\frac{d}{v}s})^2}, \tag{A7}$$

$$\tilde{c}_{A3}(s) = \tilde{c}_{B3}(s) = -\frac{\Gamma_{32}}{2\sqrt{2}}\frac{1 + \eta e^{i\phi_3}e^{-\frac{d}{v}s}}{\left(s + \frac{\Gamma_{33}}{2} + \frac{\Gamma_{33}}{2}\eta e^{i\phi_3}e^{-\frac{d}{v}s}\right)\left(s + i\omega_{23} + \frac{\Gamma_{22}}{2} + \frac{\Gamma_{22}}{2}\eta e^{i\phi_3}e^{-\frac{d}{v}s}\right) - \frac{\Gamma_{23}\Gamma_{32}}{4}(1 + \eta e^{i\phi_3}e^{-\frac{d}{v}s})^2}. \tag{A8}$$

Note that the denominators in Eqs. (A7) and (A8) are the same up to a constant shift of the Laplace variable $s \to s + i\omega_{23}$.

Similarly, for an antisymmetric initial state, i.e., $\theta = \pi/4$ and $\phi = \pi$,

$$\tilde{c}_{A2}(s) = -\tilde{c}_{B2}(s) = \frac{1}{\sqrt{2}}\frac{s - i\omega_{23} + \frac{\Gamma_{33}}{2} - \frac{\Gamma_{33}}{2}\eta e^{i\phi_2}e^{-\frac{d}{v}s}}{\left(s - i\omega_{23} + \frac{\Gamma_{33}}{2} - \frac{\Gamma_{33}}{2}\eta e^{i\phi_2}e^{-\frac{d}{v}s}\right)\left(s + \frac{\Gamma_{22}}{2} - \frac{\Gamma_{22}}{2}\eta e^{i\phi_2}e^{-\frac{d}{v}s}\right) - \frac{\Gamma_{23}\Gamma_{32}}{4}(1 - \eta e^{i\phi_2}e^{-\frac{d}{v}s})^2}, \tag{A9}$$

$$\tilde{c}_{A3}(s) = -\tilde{c}_{B3}(s) = -\frac{\Gamma_{32}}{2\sqrt{2}}\frac{1 - \eta e^{i\phi_3}e^{-\frac{d}{v}s}}{\left(s + \frac{\Gamma_{33}}{2} - \frac{\Gamma_{33}}{2}\eta e^{i\phi_3}e^{-\frac{d}{v}s}\right)\left(s + i\omega_{23} + \frac{\Gamma_{22}}{2} - \frac{\Gamma_{22}}{2}\eta e^{i\phi_3}e^{-\frac{d}{v}s}\right) - \frac{\Gamma_{23}\Gamma_{32}}{4}(1 - \eta e^{i\phi_3}e^{-\frac{d}{v}s})^2}. \tag{A10}$$

Similar to the symmetric case, the denominators on the right-hand sides of Eqs. (A9) and (A10) are the same up to a Laplace variable shift of $s \to s + i\omega_{23}$ as well.

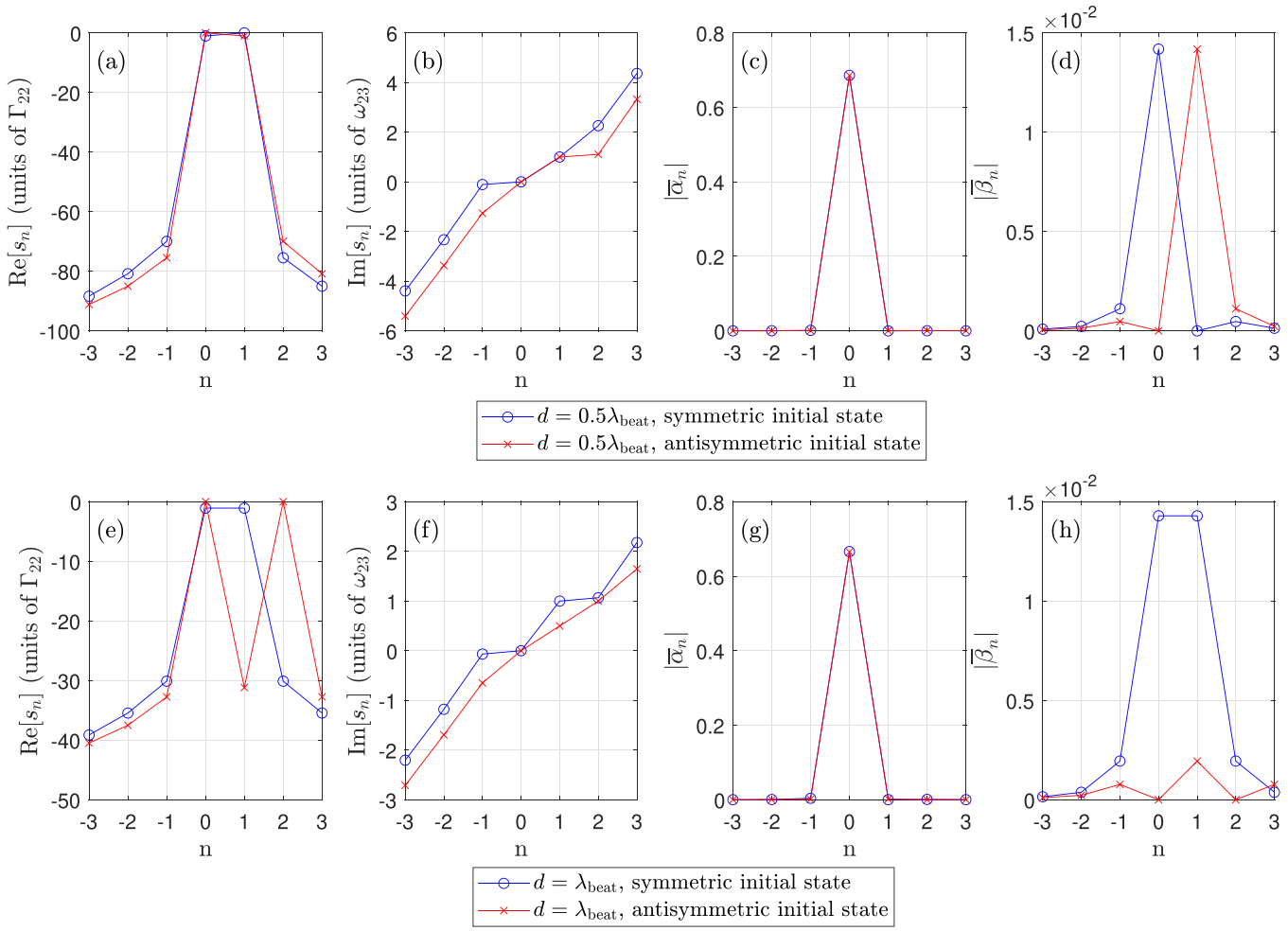

FIG. 5. Markovian regime: The poles and the corresponding coefficients for symmetric (blue circle) and antisymmetric (red x) initial states, for the separation of (a)–(d) $d = 0.5\,\lambda_{\text{beat}}$ and (e)–(h) $d = \lambda_{\text{beat}}$. (a), (e) The real part of the poles corresponds to the decay rate of each mode in units of Γ_{22} and (b), (f) the imaginary part corresponds to the frequency of the modes in units of ω_{23}. (c), (g) The coefficient $\overline{\alpha}_n$ shows the contribution of each pole to the level 2 dynamics and (d), (h) the coefficient $\overline{\beta}_n$ shows the contribution to the level 3 dynamics.

We remark that the dynamics of a general initial state in the single excitation manifold $|\Psi(0)\rangle = K_{2A}|2\rangle_A|1\rangle_B + K_{2B}|1\rangle_A|2\rangle_B + K_{3A}|3\rangle_A|1\rangle_B + K_{3B}|1\rangle_A|3\rangle_B$, with $|K_{2A}|^2 + |K_{2B}|^2 + |K_{3A}|^2 + |K_{3B}|^2 = 1$, can be obtained directly from our result. An initial excitation in $|3\rangle_A(|3\rangle_B)$ would follow the same dynamics as for the case of an initial excitation in $|2\rangle_A(|2\rangle_B)$, given by Eqs. (12) and (13), with the following substitutions:

$$\omega_{23} \leftrightarrow -\omega_{23},$$
$$\Gamma_{22} \leftrightarrow \Gamma_{33},$$
$$\Gamma_{23} \leftrightarrow \Gamma_{32}.$$

APPENDIX B: FIELD INTENSITY DYNAMICS

We consider the dynamics of the intensity radiated by the atoms as follows:

$$I(x,t) = \frac{\epsilon_0 c}{2}\langle\Psi(t)|\left[\int_0^\infty dk_1 \mathcal{E}^*_{k_1}\left\{\hat{a}^\dagger_{R,k_1}e^{-ik_1x} + \hat{a}^\dagger_{L,k_1}e^{ik_1x}\right\}e^{i\omega_1 t}\right]\left[\int_0^\infty dk_2 \mathcal{E}_{k_2}\left\{\hat{a}_{R,k_2}e^{ik_2x} + \hat{a}_{L,k_2}e^{-ik_2x}\right\}e^{-i\omega_2 t}\right]|\Psi(t)\rangle$$
$$= \frac{\epsilon_0 c|\mathcal{E}_0|^2}{2}\left|\int_0^\infty dk\left[c_R(\omega_k,t)e^{ikx} + c_L(\omega_k,t)e^{-ikx}\right]e^{-i\omega_k t}\right|^2, \tag{B1}$$

where we have assumed that $\mathcal{E}_k \approx \mathcal{E}_0$ to be constant near the atomic resonance frequency.

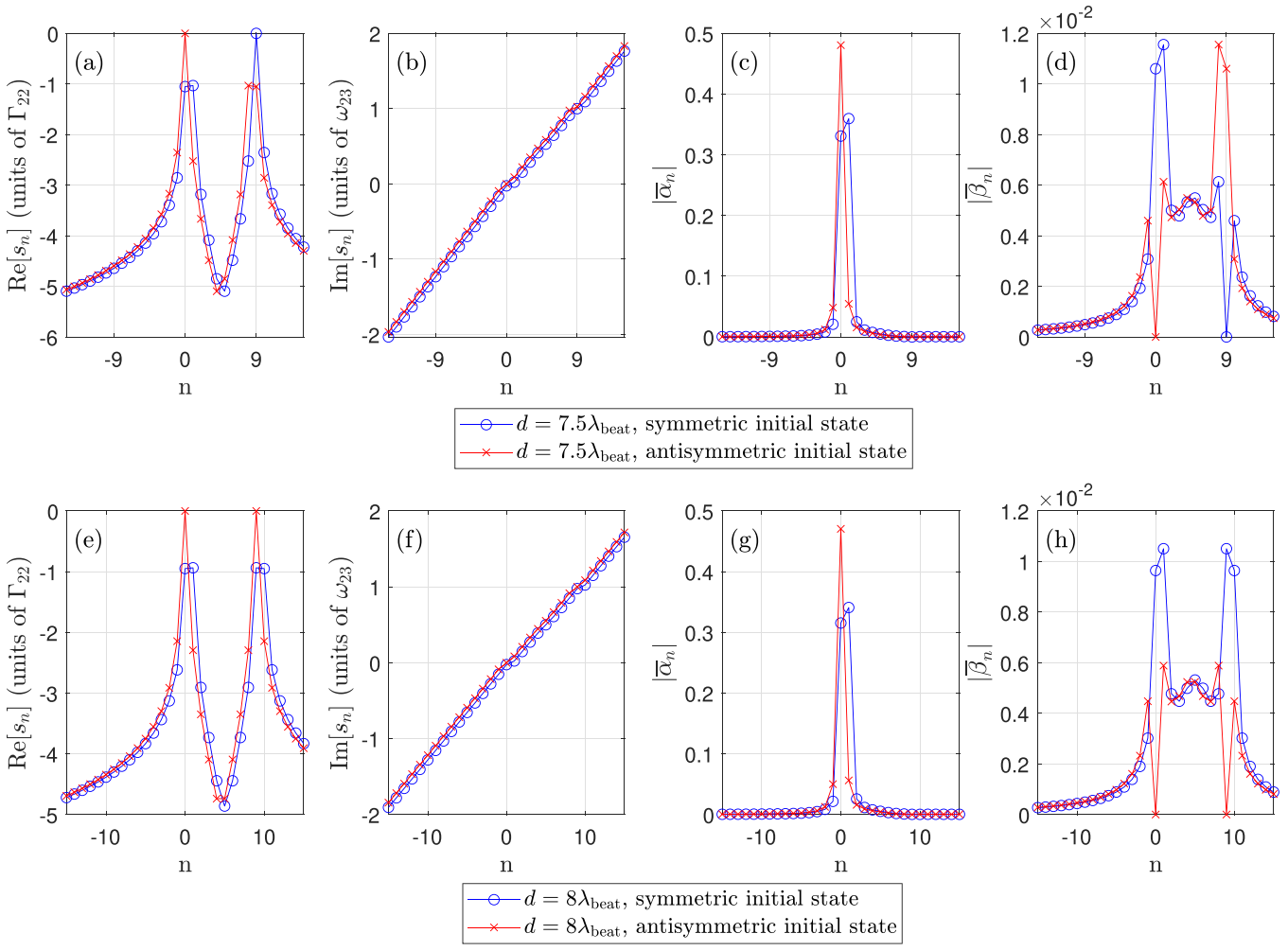

FIG. 6. Non-Markovian regime: The example of the poles and the corresponding coefficients for symmetric (blue circle) and antisymmetric (red x) initial states, for (a)–(d) $d = 7.5\,\lambda_{\text{beat}}$ and (e)–(h) $d = 8\lambda_{\text{beat}}$. (a), (e) The real part of the poles corresponds to the decay rate of each mode in units of Γ_{22} and (b), (f) the imaginary part corresponds to the frequency of the modes in units of ω_{23}. (c), (g) The coefficient $\overline{\alpha}_n$ shows the contribution of each pole to the level 2 dynamics and (d), (h) the coefficient $\overline{\beta}_n$ shows the contribution to the level 3 dynamics.

We can derive the excitation amplitudes of the field modes from Eq. (6) and (7) as follows:

$$c_R(\omega_k, t) = i \int_0^t d\tau \sum_{m=A,B} \sum_{j=2,3} g_j(\omega_k) e^{-i(\omega_{j1}-\omega_k)\tau} c_{m,j}(\tau) e^{-ikx_m}, \tag{B2}$$

$$c_L(\omega_k, t) = i \int_0^t d\tau \sum_{m=A,B} \sum_{j=2,3} g_j(\omega_k) e^{-i(\omega_{j1}-\omega_k)\tau} c_{m,j}(\tau) e^{ikx_m}. \tag{B3}$$

Then one can simplify the intensity expression [Eq. (B1)] in terms of the atomic coefficients as follows:

$$I(x,t) = \frac{\epsilon_0 c |\mathcal{E}_0|^2}{4\pi} \left| \int d\omega e^{-i\omega t} \left[\int_0^t d\tau \sum_{j=2,3} g_j \{ c_{Aj}(\tau) e^{i\omega(-x+x_A)/v} + c_{Bj}(\tau) e^{i\omega(-x+x_B)/v} \right.\right.$$
$$+ c_{Aj}(\tau) e^{-i\omega(-x+x_A)/v}$$
$$\left.\left. + c_{Bj}(\tau) e^{-i\omega(-x+x_B)/v} \} e^{i(\omega-\omega_{j1})\tau} \right] \right|^2, \tag{B4}$$

where we have used Eqs. (B2) and (B3) to determine the field excitation amplitudes in terms of those of the atoms. Performing first the integral over frequency and subsequently the integral over time leads to Eq. (19).

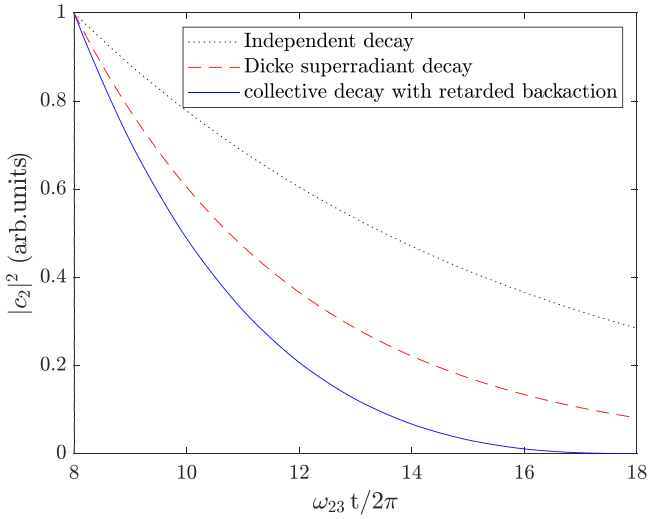

FIG. 7. The dynamics of the population in level 2 of the initial symmetric state of atoms for three scenarios: independent decay ($d = \infty$, dotted black), Dicke superradiance ($d = 0$, dashed red), and superduperradiance, i.e., the non-Markovian collective decay with retarded backaction ($d = 8\lambda_{\text{beat}}$, solid blue), each rescaled to 1 at $t = 8\lambda_{\text{beat}}/v$ for clear comparison.

APPENDIX C: POLES FOR THE MARKOVIAN AND THE NON-MARKOVIAN EXAMPLES

The poles s_n and the corresponding coefficients $\alpha_n^{(\pm)}$ and $\beta_n^{(\pm)}$ in Eqs. (12) and (13) determine the atomic and the field dynamics. However, the coefficients $\alpha_n^{(\pm)}$ and $\beta_n^{(\pm)}$ also account for the higher eigenfrequencies that cause an abrupt change at $t = d/v$, arising due to the time-delayed feedback. Since we are interested in the dynamics after $t = d/v$, we redefine the following coefficients:

$$\overline{\alpha}_n \equiv \alpha_n e^{s_n d/v}, \tag{C1}$$

$$\overline{\beta}_n \equiv \beta_n e^{s_n d/v}. \tag{C2}$$

The dynamics after $t = d/v$ is thus described as

$$c_{A2}(t) = \sum_{n=-\infty}^{\infty} \overline{\alpha}_n e^{s_n (t-d/v)}, \tag{C3}$$

$$c_{A3}(t) = \sum_{n=-\infty}^{\infty} \overline{\beta}_n e^{(s_n - i\omega_{23})(t-d/v)}. \tag{C4}$$

$\overline{\alpha}_n$ and $\overline{\beta}_n$ do not consider the high-frequency components constituting the abrupt change at $t = d/v$, and only account for the dynamics in the regime $t > d/v$.

Figures 5 and 6 show the poles s_n and the corresponding coefficients $\overline{\alpha}_n$ and $\overline{\beta}_n$ for Markovian and non-Markovian regimes, respectively. The real part of the poles represents the collective decay rate and the imaginary part represents collective shift of energy in the eigenmodes. We see that in the Markovian regime (Fig. 5) the high-frequency and fast decaying modes have negligible contribution. In contrast, the non-Markovian regime (Fig. 6) shows that the dominant poles occur in the range of frequencies between zero and ω_{23}, and decay rates that are enhanced beyond the Markovian limit.

APPENDIX D: COMPARISON OF SUPERDUPERRADIANCE AND DICKE SUPERRADIANCE IN LEVEL 2 DYNAMICS

The enhancement of decay rate of level 2 population for symmetrically correlated emitters in a non-Markovian regime exceeds the standard Dicke superradiant decay rate, whereas

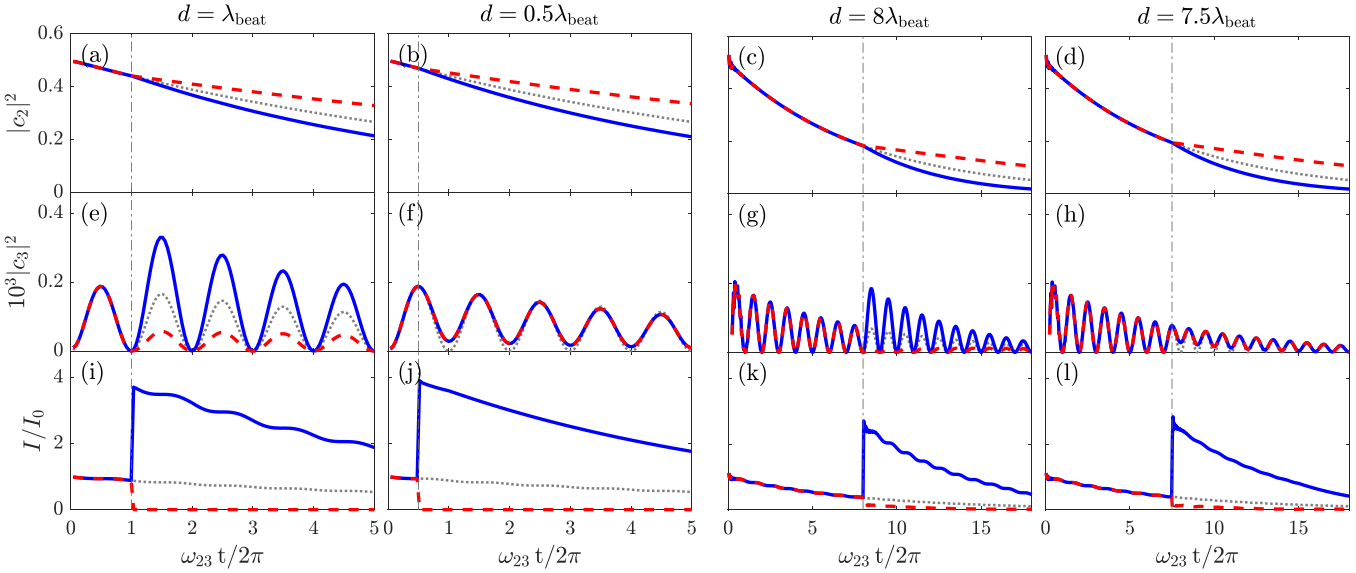

FIG. 8. The atom-field dynamics for coupling efficiency $\eta = 0.4$: (a)–(d) level 2 dynamics, (e)–(h) level 3 dynamics, and (i)–(l) field dynamics measured at $x \to x_B^+$ for interatomic separations (a), (e), (i) $d = \lambda_{\text{beat}}$, (b), (f), (j) $d = 0.5\lambda_{\text{beat}}$, (c), (g), (k) $d = 8\lambda_{\text{beat}}$, and (d), (h), (l) $d = 7.5\lambda_{\text{beat}}$. The solid blue curves are for the symmetric initial state, and the dashed red curves are for the antisymmetric initial state. The vertical dash-dotted lines indicate the times when the field emitted from one atom reaches the other atom. For comparison the single atom dynamics is drawn with the dotted gray lines. The level 3 population is scaled by a factor of 10^3 for clarity of illustration.

it is hard to tell just by looking at Figs. 4(a) and 4(b). Figure 7 shows a direct comparison of non-Markovian enhancement of decay for the case of $d = 8\lambda_{\text{beat}}$, to the standard Dicke superradiant decay and independent decay, demonstrating that retarded backaction may lead to a faster-than-superradiance decay.

APPENDIX E: MARKOVIAN AND NON-MARKOVIAN DYNAMICS FOR IMPERFECT COUPLING EFFICIENCY

The example of imperfect coupling efficiency of $\eta = 0.4$ is shown in Fig. 8. The general effect of having a finite coupling efficiency is that the interference between different atoms observed at the separation time is mitigated. In consequence, the level 2 dynamics shows reduced enhancement and suppression of decay rates for symmetric and antisymmetric initial states, respectively. Similarly, the level 3 dynamics for $d = n\lambda_{\text{beat}}$ shows less enhancement and suppression of quantum beats for symmetric and antisymmetric initial states, respectively. In the level 3 dynamics for $d = (n + \frac{1}{2})\lambda_{\text{beat}}$, destructive interference due to the out-of-phase photon from the other atom is also reduced. As a result, the intensity of light emitted from the system shows less enhancement or suppression of the decay rate and the quantum beats.

[1] E. T. Jaynes, in *Foundations of Radiation Theory and Quantum Electrodynamics*, edited by A. O. Barut (Springer, New York, 1980), pp. 37–43.

[2] R. H. Dicke, Phys. Rev. **93**, 99 (1954).

[3] G. S. Agarwal, Phys. Rev. A **15**, 2380 (1977).

[4] H. S. Han, A. Lee, K. Sinha, F. K. Fatemi, and S. L. Rolston, Phys. Rev. Lett. **127**, 073604 (2021).

[5] S. Haroche, in *High-Resolution Laser Spectroscopy*, edited by K. Shimoda (Springer-Verlag, Berlin, 1976), pp. 253–313.

[6] M. Gross, C. Fabre, P. Pillet, and S. Haroche, Phys. Rev. Lett. **36**, 1035 (1976).

[7] M. Gross and S. Haroche, Phys. Rep. **93**, 301 (1982).

[8] N. Skribanowitz, I. P. Herman, J. C. MacGillivray, and M. S. Feld, Phys. Rev. Lett. **30**, 309 (1973).

[9] D. Pavolini, A. Crubellier, P. Pillet, L. Cabaret, and S. Liberman, Phys. Rev. Lett. **54**, 1917 (1985).

[10] R. G. DeVoe and R. G. Brewer, Phys. Rev. Lett. **76**, 2049 (1996).

[11] A. S. Sheremet, M. I. Petrov, I. V. Iorsh, A. V. Poshakinskiy, and A. N. Poddubny, arXiv:2103.06824.

[12] V. A. Pivovarov, L. V. Gerasimov, J. Berroir, T. Ray, J. Laurat, A. Urvoy, and D. V. Kupriyanov, Phys. Rev. A **103**, 043716 (2021).

[13] A. Asenjo-Garcia, M. Moreno-Cardoner, A. Albrecht, H. J. Kimble, and D. E. Chang, Phys. Rev. X **7**, 031024 (2017).

[14] A. F. van Loo, A. Fedorov, K. Lalumiére, B. C. Sanders, A. Blais, and A. Wallraff, Science **342**, 1494 (2013).

[15] Y. Li and C. Argyropoulos, Opt. Express **24**, 26696 (2016).

[16] P. Solano, P. Barberis-Blostein, F. K. Fatemi, L. A. Orozco, and S. L. Rolston, Nat. Commun. **8**, 1857 (2017).

[17] J.-H. Kim, S. Aghaeimeibodi, C. J. K. Richardson, R. P. Leavitt, and E. Waks, Nano Lett. **18**, 4734 (2018).

[18] W. D. Newman, C. L. Cortes, A. Afshar, K. Cadien, A. Meldrum, R. Fedosejevs, and Z. Jacob, Sci. Adv. **4**, eaar5278 (2018).

[19] A. K. Boddeti, J. Guan, T. Sentz, X. Juarez, W. Newman, C. Cortes, T. W. Odom, and Z. Jacob, Nano Lett. **22**, 22 (2022).

[20] R. Pennetta, M. Blaha, A. Johnson, D. Lechner, P. Schneeweiss, J. Volz, and A. Rauschenbeutel, Phys. Rev. Lett. **128**, 073601 (2022).

[21] M. Zanner, T. Orell, C. M. F. Schneider, R. Albert, S. Oleschko, M. L. Juan, M. Silveri, and G. Kirchmair, Nat. Phys. **18**, 538 (2022).

[22] P. Solano, J. A. Grover, J. E. Hoffman, S. Ravets, F. K. Fatemi, L. A. Orozco, and S. L. Rolston, Adv. At. Mol. Opt. Phys. **66**, 439 (2017).

[23] D. E. Chang, L. Jiang, A. V. Gorshkov, and H. J. Kimble, New J. Phys. **14**, 063003 (2012).

[24] N. V. Corzo, B. Gouraud, A. Chandra, A. Goban, A. S. Sheremet, D. V. Kupriyanov, and J. Laurat, Phys. Rev. Lett. **117**, 133603 (2016).

[25] M. Mirhosseini, E. Kim, X. Zhang, A. Sipahigil, P. B. Dieterle, A. J. Keller, A. Asenjo-Garcia, D. E. Chang, and O. Painter, Nature (London) **569**, 692 (2019).

[26] L. Ostermann, H. Ritsch, and C. Genes, Phys. Rev. Lett. **111**, 123601 (2013).

[27] L. Henriet, J. S. Douglas, D. E. Chang, and A. Albrecht, Phys. Rev. A **99**, 023802 (2019).

[28] M. T. Manzoni, M. Moreno-Cardoner, A. Asenjo-Garcia, J. V. Porto, A. V. Gorshkov, and D. E. Chang, New J. Phys. **20**, 083048 (2018).

[29] F. Dinç and A. M. Brańczyk, Phys. Rev. Res. **1**, 032042(R) (2019).

[30] S. Rist, J. Eschner, M. Hennrich, and G. Morigi, Phys. Rev. A **78**, 013808 (2008).

[31] K. Sinha, A. González-Tudela, Y. Lu, and P. Solano, Phys. Rev. A **102**, 043718 (2020).

[32] K. Sinha, P. Meystre, E. A. Goldschmidt, F. K. Fatemi, S. L. Rolston, and P. Solano, Phys. Rev. Lett. **124**, 043603 (2020).

[33] K. Sinha, P. Meystre, and P. Solano, Nanophot. Mater. Dev. Syst. **11091**, 53 (2019).

[34] G. Calajó, Yao-Lung L. Fang, H. U. Baranger, and F. Ciccarello, Phys. Rev. Lett. **122**, 073601 (2019).

[35] R. Trivedi, D. Malz, S. Sun, S. Fan, and J. Vučković, Phys. Rev. A **104**, 013705 (2021).

[36] P. Yao and S. Hughes, Opt. Express **17**, 11505 (2009).

[37] G. C. Hegerfeldt and M. B. Plenio, Quantum Opt. **6**, 15 (1994).

[38] S. J. Srinivasan, A. J. Hoffman, J. M. Gambetta, and A. A. Houck, Phys. Rev. Lett. **106**, 083601 (2011).

[39] F. Dinç, A. M. Brańczyk, and I. Ercan, Quantum **3**, 213 (2019).

[40] P. Solano, P. Barberis-Blostein, and K. Sinha, arXiv:2108.12951.

[41] A. Asenjo-Garcia, H. J. Kimble, and D. E. Chang, Proc. Natl. Acad. Sci. USA **116**, 25503 (2019).

[42] N. J. Cerf, M. Bourennane, A. Karlsson, and N. Gisin, Phys. Rev. Lett. **88**, 127902 (2002).

[43] A. Vaziri, G. Weihs, and A. Zeilinger, Phys. Rev. Lett. **89**, 240401 (2002).

[44] H. Bechmann-Pasquinucci and W. Tittel, Phys. Rev. A **61**, 062308 (2000).